

## **DEVELOPMENT OF ALUMINIUM ROOFING SHEETS FROM WASTE BEVERAGE CANS**

**Akindapo J. O<sup>1</sup>, Dayak M. J<sup>1</sup>, Orueri D. U<sup>1</sup>.**

<sup>1</sup>Department of Mechanical Engineering, Nigerian Defence Academy, Kaduna

---

### **Abstract**

The research aimed to develop aluminum roofing sheets utilizing waste beverage cans, with a focus on minimizing costs and energy consumption. This initiative adhered to ASTM and ISO standard measures and procedures. Waste beverage cans underwent analysis and were compared with control sheets. Subsequently, they were manually melted, alloyed, and cast before being rolled to achieve the desired thickness and enhance specific properties. The resulting sheets were then corrugated. Upon analysis, the produced aluminum sheets exhibited promising characteristics. The corrosion penetration rate was measured at 0.045mm/yr, with a Rockwell hardness number of 55.1 and an indentation depth of 0.1498mm. Moreover, the average impact strength stood at 2.05, with a tensile strength of 71.69Mpa, yield strength of 25.65Mpa, and young modulus of 2596.43Mpa. The findings indicated a significant enhancement in the properties of the aluminum sheets manufactured from waste beverage cans. This underscored the feasibility of utilizing such cans in producing aluminum roofing sheets. Based on the results, it is recommended to further explore and refine the manufacturing process for aluminum roofing sheets from waste beverage cans. Additionally, continued adherence to ASTM and ISO standards is essential for ensuring product quality and reliability.

**Keywords:** Aluminium roofing sheet, Waste beverage can, Corrosion resistance, Material properties, Recycling.

---

### **1. INTRODUCTION**

The evolution of roofing materials and techniques has been a gradual process spanning centuries. Although the significant growth in the roofing industry has occurred primarily within the last two centuries, the roots of roofing can be traced back much further. Notably, the production of

Dreadnought clay tiles in 1805 marked a significant milestone, while early industrial roofing, though lacking in insulation, boasted effective rainwater drainage systems (Obam & Taku, 2015).

Concrete tile roofing emerged a century later, further diversifying the landscape of roofing

materials. Yet, throughout history, roofing styles, whether in America or abroad, were heavily influenced by regional material availability. Today, roofing materials have evolved to encompass a wide range of options, including metal sheets, slates, and felts, which are commonly utilized in construction (Oboh *et al*, 2017).

The future trajectory of the roofing industry remains uncertain, but advancements in technology continue to shape its course indefinitely. Beyond mere functionality, the roof plays a pivotal role in enhancing the aesthetic appeal of a building when designed thoughtfully. Moreover, it constitutes a significant portion, approximately 8%, of the total construction costs (Ramakrishna *et al*, 2011).

In many developing countries, including those in the third world, asbestos cement-based roofing and lightweight materials such as long-span aluminum and aluminum-zinc are prevalent choices for residential and industrial buildings (Oladele *et al*, 2009).

Metal roofing sheets, including those made from aluminum, zinc, and galvanized coatings, demonstrate unique properties such as thermal expansion and durability. Aluminum, in particular, stands out for its lightweight nature, corrosion resistance, and recyclability. Its versatility extends to applications in roofing sheets and beverage cans alike, owing to its remarkable properties (Obam & Taku, 2015).

While primary aluminum production from bauxite ore is time-consuming, recycling aluminum offers a sustainable alternative. Not only does aluminum recycling conserve energy, but it also mitigates environmental impact and generates revenue for recyclers (Kiffaya & Layla, 2008; Manuela, 2017).

This research paper aims to explore the utilization of waste aluminum beverage cans in the production of aluminum roofing sheets through

recycling processes. By circumventing primary production from bauxite, this study seeks to demonstrate the feasibility and benefits of recycling aluminum cans for roofing sheet manufacturing. Thus, the primary focus of this study lies in the recycling of aluminum beverage cans and their transformation into aluminum roofing sheets.

## 2. LITERATURE REVIEW

This paper by Deng *et al* (2019) explored the advantages and challenges of using additive manufacturing (AM) for aluminum alloys in aeronautics, focusing on defects, microstructure, and mechanical properties.

This study by Xu *et al* (2020) discussed the use of wire-based AM processes for producing large aluminum components, emphasizing the cost-competitiveness and efficiency of wire and arc additive manufacturing (WAAM).

This review by Pragana *et al* (2021) focused on the rapid production capabilities of wire and arc additive manufacturing (WAAM) for Al-Li alloys, discussing wire production processes and the role of alloying elements.

This review by Zhang *et al* (2020) highlighted the development of new aluminum alloys tailored for laser powder bed fusion (LPBF), addressing challenges like low laser absorption and thermal conductivity.

This paper by Hu *et al* (2019) examined the MELD process for manufacturing aluminum matrix composites, discussing the benefits of solid-state AM for producing high-strength aluminum components.

This study by Santos and Filho (2021) investigated the fabrication techniques and mechanical properties of high-performance aluminum alloy components produced through AM.



This paper by Sun *et al* (2020) explored various AM techniques for improving the properties of aluminum alloys, including their mechanical strength and corrosion resistance.

This article by Williams *et al* (2016) reviewed the current advances and challenges in the additive manufacturing of aluminum alloys, focusing on process optimization and material properties.

This research by Qiu *et al* (2019) investigated how AM processes affect the microstructure and mechanical properties of aluminum alloys.

This comprehensive review by Kumar *et al* (2020) discussed recent innovations in aluminum alloy manufacturing, with a focus on additive manufacturing techniques and their industrial applications.

Varone (2023) in his study explored the use of additive manufacturing (AM) technologies for producing aluminum alloys in the aerospace sector, focusing on the benefits of weight reduction and improved mechanical properties. The study also addressed the challenges related to defects, microstructure, and post-processing treatments.

The article by Kane (2024) discussed the advancements in aluminum technology, particularly the development of new alloys with improved corrosion resistance and the integration of recycled aluminum. It also highlighted the energy-intensive nature of aluminum production and the potential of AI in enhancing production efficiency.

Smith and Lee (2021) in their research examined the mechanical properties of aluminum roofing sheets, focusing on enhancements in tensile strength and corrosion resistance through the incorporation of various alloying elements and surface treatments.

The study by Garcia and Thompson (2022) explored the recycling processes for aluminum and the production of sustainable roofing materials. It emphasized the environmental benefits and economic viability of using recycled aluminum in construction.

This research by Patel and Wang (2020) focused on the development of aluminum alloys with enhanced corrosion resistance for roofing applications. The study investigated various alloying elements and coating technologies to improve durability.

The paper by Davis and Wilson (2019) analyzed the performance of contemporary aluminum roofing systems, including their thermal properties, durability, and resistance to environmental factors. The study highlighted innovations in design and materials that enhance the overall efficiency of aluminum roofing.

### 3. MATERIALS AND METHODS

#### 3.1 Materials

The following materials were used in this research work;

- i. Beverage scrap cans
- ii. Aluminium corrugated roofing sheet (control)
- iii. Pure aluminium

#### 3.2 Equipment

The list of equipment used for this research are presented in Table 1.



**Table 1: List of Equipment Used**

S/N	NAME	SPECIFICATION	MODEL
1.	X-Ray fluorescence spectrometer (XRF)	Wavelength-dispersive XRF	Bruker S2, Ranger XRF Spectrometer
2.	Wooden mold		Hand made
3.	Impact testing machine		Cat. Nr. 412
4.	Tensile testing machine		WDW-1000KN
5.	Crucible Furnace	Locally made with a blower of 3.5kw capacity	None
6.	Infrared pyrometer	Fiber optics sensitive laser	E-series
7.	Manual Rolling Machine	Thickness of up to 5mm and width of 1000mm	WALTONS Industrial 3-in-1/30 sheet metal break, 30-inch shear brake roll machine
8.	Aluminium roofing sheet Corrugating Machine	Adjustable corrugation patterns, roll forming, cutting mechanisms	Bradbury robust panel Ag panel corrugating machine
9.	Coating Oven for aluminium sheets	Precise temperature control, efficient heating elements	Nordson encore LT Powder coating
10.	Precision Digital scale machine	Few 100g with tare functions and calibration	AWS series precision scales
11.	Hardness Testing Machine		CRBD MAT25



Solid works software was employed for the design of the pattern, mold and other shapes for test.

### 3.3 Methods

In the production of aluminium roofing sheets from scrap aluminium beverage cans, the following procedures were followed;

#### 3.3.1 Determination of the Chemical Composition of Aluminium Roofing Sheet and the Aluminium Cans

Samples of both the roofing sheets and the aluminum cans were obtained and subjected to chemical composition analysis using an X-ray Fluorescence (XRF) machine. This step was crucial as it unveiled the specific alloying elements required to be incorporated into the aluminum cans to achieve a composition similar to that of the control sample aluminum roofing sheet.

#### 2.3.2 Determination of the Quantity of Aluminium Cans and Pure Aluminium Needed

The quantity of aluminium cans to be used was determined from the relation below;

Volume of plate = Length of plate × breadth of plate × thickness of plate.....1

Total mass of cans and pure aluminum needed per plate = 1406g + 390.3g + 32.46g + 282.11g = 2110.87g. Two samples of the plates were produced. Therefore, a combination of pure aluminum and aluminum cans gives a total of 4221.74g which is approximately 4222g.

#### 3.3.3 Design of Mold for Casting

To facilitate the design of the casting mold based on the provided parameters, SolidWorks software was employed to generate the required designs along with their respective specifications. A skeletal design for both the top and bottom sections of the wooden mold box was created, as illustrated in Figures 1 and 2

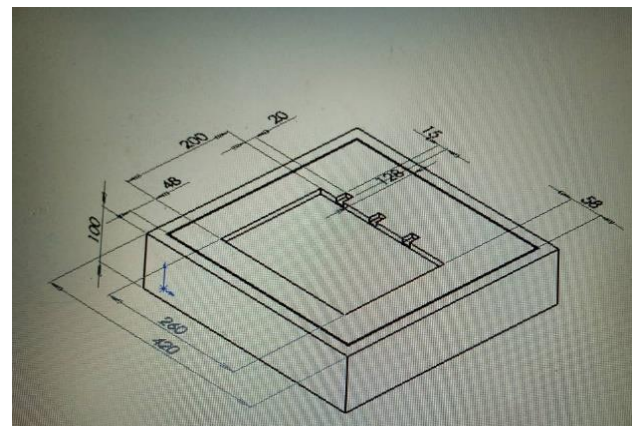
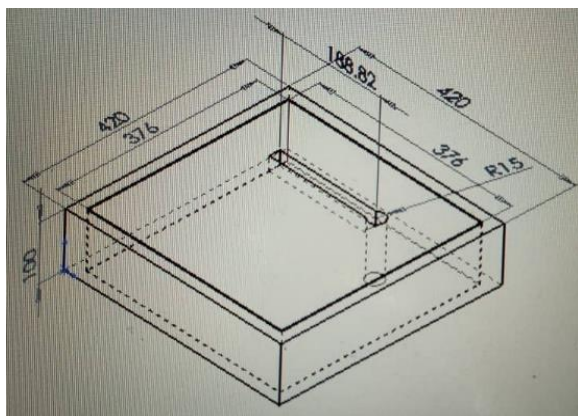


**Figure 1:** Skeletal top part of the wooden mold **Figure 2:** Skeletal bottom part of the mold

Then the skeletal designs were solidified as seen in Figures 3 and 4

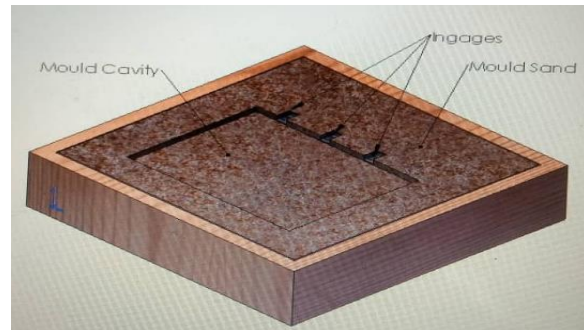
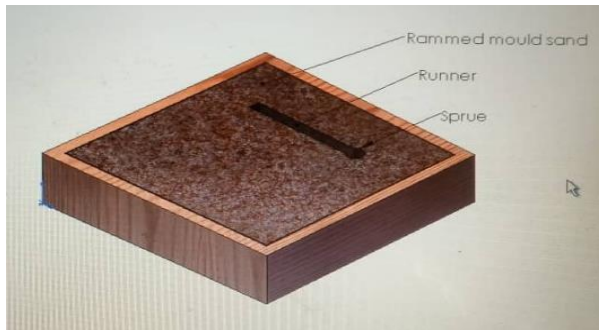


**Figure 3:** Solidified top part of the mold box

**Figure 4:** Solidified bottom part of the mold box

The design of the pattern coupled with a sprue, ingates and a runner with their specifications is shown in Figure 5.

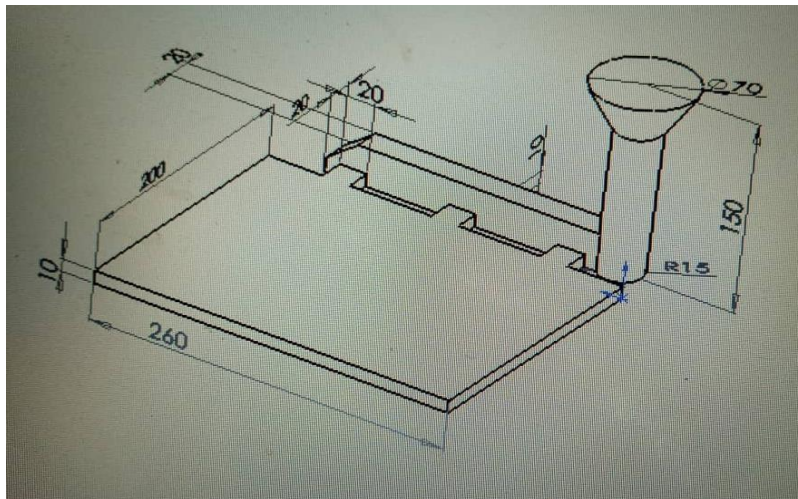


**Figure 5:** Pattern coupled with a sprue, ingate and runner

### 3.3.4 Charge Calculations

To determine the optimal combination of alloying elements required for the crucible furnace to achieve the desired alloy, a charge calculation was performed. This calculation indicated that to attain the target alloy, half of the composition should consist of high-purity aluminum (99.9% Al), while the remaining half should comprise aluminum cans. This adjustment is necessary because aluminum cans contain a higher percentage of impurities and alloying elements, such as magnesium and manganese, compared to

the sample roofing sheet. Consequently, adding high-purity aluminum to the melted cans reduces the percentage of these alloying elements, aligning the final alloy composition with the requirements for the roofing sheet. Thus, only high-purity aluminum was included as an alloying element. As a result, the aluminum cans sourced for this research must weigh over 2500g to ensure an adequate supply for the experiment. The detailed charge calculation is provided below.

**Table 2: Charge composition**

Charge Materials		Aluminium Can	Pure Aluminium	Total
Chemical	Value	1250g	1250g	2500g
Aluminium	Percentage	95.9	99.8	97.85%
	Mass	1198.75	1247.5	2446.25g
Silicon	Percentage	0.29	-	0.145%
	Mass	3.625	-	3.625g
Copper	Percentage	0.307	-	0.1535%
	Mass	3.8375	-	3.8375g
Magnesium	Percentage	1.14	-	0.57%
	Mass	14.25	-	14.25g
Manganese	Percentage	1.22	-	0.61%
	Mass	15.25	-	15.25g
Iron	Percentage	0.6	-	0.000144%
	Mass	0.0036	-	0.0036
Zinc	Percentage	0.094	-	0.047
	Mass	1.175	-	1.175

### 3.3.5 Sourcing, Crushing and Weighing of Aluminium Cans

The cans selected for this research were locally sourced, specifically Maltina cans. Upon acquisition of an ample quantity of cans, they were crushed to maximize space before being weighed using a digital weighing machine. The total weight of the sourced cans amounted to approximately 3000g, which proved to be adequate for the research, allowing for the production of two samples. Additionally, 3000g of pure aluminum was procured for the experiment.

### 3.3.6 Production of Mold Box and Pattern

Utilizing the dimensions provided in Figures 3 to 5 for the mold and pattern, a wooden mold was crafted to ensure optimal results. The pattern, measuring 20cm by 26cm by 1cm, was fashioned from a flat wooden material with a smooth surface. It was intentionally fabricated slightly larger than the final product to account for contraction allowance during the casting process.



### 3.3.7 Production of the Mold

The casting method employed in this work was sand casting utilizing a wooden mold consisting of the cope and drag components.

Initially, the lower portion of the mold box (drag) was positioned on a level surface and filled with molding sand to its brim, followed by vigorous ramming to ensure the sand was densely packed. Subsequently, the wooden pattern was placed atop the compacted molding sand and similarly rammed into position to align horizontally with the sand surface. Parting sand was then applied to create a separation line between the cope and drag.

The cope component was subsequently positioned over the drag, ensuring a seamless fit. The design included provisions for metal entry into the cavity through the sprue, ingate, and runner channels.

Next, the cope was filled with molding sand up to the brim, while simultaneously creating a channel for the sprue using an iron pipe directly connected to the designed runner. The sand was then vigorously rammed again to ensure compactness, and a pouring cup was formed during this process. Subsequently, the cope was cautiously separated from the drag, and the patterns for the runner, ingates, and sprue were gradually removed to reveal the desired cavity, as depicted in Plate 1, for both the core and drag components.



**Plate 1: Sand filled cope and drag with cavity created**

The same process was adopted for the production of the second mold.

### 3.3.8 Casting of aluminium plate

The casting process was conducted utilizing a locally fabricated crucible furnace. This type of furnace employs a refractory crucible designed to withstand extremely high temperatures without succumbing to melting. The decision to utilize a crucible furnace was based on several factors:

- i. The relatively low melting point of the aluminum alloy.
- ii. The quantity of metal to be melted was not substantial.
- iii. Melting metal in a crucible furnace provides protection from direct

exposure to the heat source, thereby preserving its metallurgical integrity and minimizing melt losses.

- iv. Utilizing a crucible furnace helps prevent local overheating of the metal, thereby reducing oxidation and minimizing the volatilization of charge constituents.

The crucible furnace utilized (refer to Plate 2) is equipped with a blower featuring a controller valve for temperature regulation. This blower is electrically powered, and it supplies air through a pipe to the combustion chamber, which is fueled by charcoal. Additionally, the furnace includes a crucible pot for containing the metal charge.





**Plate 2: Crucible Furnace**

Initially, the combustion chamber underwent thorough cleaning before being filled with the designated fuel, charcoal. Proper filling was ensured, followed by ignition to fire up the charcoal. Subsequently, the crucible pot was carefully positioned atop the combustion chamber. The charcoal was allowed to ignite fully before activating the blower to ensure even distribution of heat throughout the combustion chamber.

Once the crucible pot reached the desired temperature, it was gradually loaded with a mixture comprising 1250g of pure aluminum and 1250g of crushed aluminum cans, then securely covered. As previously discussed, only pure aluminum was added to the crucible, as the goal was to adjust the composition of the aluminum cans by reducing the percentages of certain key elements to align with the desired composition for the roofing sheet.

The combustion chamber was fired to reach a temperature of 660°C, the melting point of aluminum. Temperature control was managed through the regulator on the blower, while monitoring was conducted using an infrared pyrometer. Upon reaching the target temperature, the aluminum began to melt almost instantly.



**Plate 3: Process of Melting**

After approximately a minute, ensuring complete melting of the aluminum, any impurities, referred to as dross, that settled on the surface of the molten metal were carefully removed using a sieve with an extended handle.

As the melting process commenced (refer to Plate 3), the mold was carefully repositioned near the melting area. The cope was then meticulously placed onto the drag, ensuring accurate and secure alignment to prevent any potential spillage or overflow. Once the metal was confirmed to be completely molten, the crucible pot containing the molten metal was cautiously removed from the combustion chamber using tongs to avoid spillage. The molten metal was immediately poured into the prepared pattern through the pouring cup (refer to Plate 4) until all cavities were filled, after which it was left to solidify for a duration of 20 minutes.

During the solidification of the first plate, the second batch of 1250g of aluminum cans and 1250g of pure aluminum were introduced into the crucible. They were allowed to melt completely at the same temperature as the first plate and then poured into the second mold, where they were also left to solidify. The casting process is depicted in Plates 4 and 5.



**Plate 4: Pouring of molten metal into 1<sup>st</sup> cavity**

Following a 25-minute duration, the molten metal had sufficiently filled the cavities or patterns within the mold and solidified. The mold was then disassembled gradually, starting with the separation of the cope from the drag, with the plate attached to the cope. Subsequently, the pattern was removed from the cope, resulting in the finalized product, as depicted in Plate 6.



**Plate 5: Pouring of molten metal into 2nd cavity**

were cut off from the plate with a hacksaw to leave only the 26cm by 20cm by 1cm plate. After that, a metal analysis was carried out on the finished product using the X-Ray fluorescence machine to determine the composition. The result of the analysis is given in Table 3.

### 3.4 Experimentation

The following experiments were conducted on the produced 3mm aluminium plate before the rolling process was carried out on it. This was carried out in order to determine the various mechanical properties of the aluminium.

#### 3.4.1 Hardness Test

The hardness test was conducted using the indentec Universal Hardness Testing Machine (UHTM) with the rockwell hardness scale. The sample to be used was designed according to the ASTM Standards (ASTM E-18) dimensions for hardness test. The indenter used was a steel ball of 1/16 inch with a pre-load of 10kgf and a major load of 100kgf according to ASTM E-18 and ISO 6508 and then the rockwell hardness number



**Plate 6: Product after casting with the ingate and the runner still attached**

It was allowed to cool off completely, the excesses such as the runner, ingate and sprue

obtained. The test was conducted three times and the mean determined.

### 3.4.2 Impact Strength Test

The Charpy impact test was used to determine the resistance capacity of the aluminium bar specimen against sudden impact load of a pendulum which swung from a certain height using the impact testing machine (Plate 3.25). Impact tests were conducted in accordance with ASTM A23 and ISO 148-1. The pendulum was swung at a capacity of 15J and 25J.

### 3.4.3 Tensile Strength Test

The tensile strength test was carried out in accordance with ASTM B557 Standard and ISO 6892-1. The universal electronic testing machine of capacity 1000kN was used to carry out the work in order to evaluate the tensile strength and ductility of the Al alloy test specimen. The sample produced was firmly gripped on the testing machine and the machine calibrated and set to zero to avoid any errors. The testing parameters such as test speed and gauge length were set according to ASTM B557. The machine was started and the load applied to the aluminium specimen. All the necessary readings were recorded and tabulated. The line graph was displayed on the computer monitor which was connected to the equipment. The instrument was comprised of a DC servo motor drive and digital indicating unit.

### 3.4.4 Corrosion Resistance Test

The method used to check for the corrosion resistance was the corrosion rate assessment through weight loss due to corrosion after removal of all adherent coating and, or corrosion products on a metal, using standard combined chemical (or electrochemical) and mechanical cleaning operations or some other method that will not cause further attack in the corrosion process, or by making a proper correction for losses in the cleaning process. The aluminium

specimen was first pre-treated by polishing with sand paper, it was then washed with distilled water available and cleaned with a clean cloth. It was then weighed on the weighing balance and the value noted and then inserted into the test solution which was sodium hydroxide. After 45 hours, it was removed, cleaned and weighed again with the figure noted.

### 3.5 Rolling process

The initially produced plate was too thick to be suitable for roofing sheets. Consequently, it required a reduction in thickness to ensure it could be easily corrugated for roofing purposes. While various methods exist for reducing plate thickness to less than 1cm, such as rolling and milling, the rolling process was chosen for this research due to its demonstrated ability in not only reducing plate thickness but also enhancing its mechanical and chemical properties.

Two plates were cast and subjected to both hot and cold rolling processes using a manual rolling machine. Hot rolling, a widely recognized technique for substantial thickness reduction before cold rolling, was employed. The first step involved heating the plate in a local furnace to a temperature approximating the hot rolling temperature of aluminum, which is around 396°C. This temperature was determined by multiplying the metal's melting point by 0.6, which for aluminum exceeds 300°C. The plate was heated above its recrystallization temperature, passed through the manual roller five times, and then reheated as necessary until its thickness was reduced from 10mm to approximately 3mm. The same process was applied to the second plate, achieving similar thickness reduction.

Once cooled completely, the plates, now both 3mm thick, underwent cold rolling to further meet ASTM Standards for sheets and plates. They were passed through the manual roller six times, reducing their thickness to about 2mm and

improving their properties. However, cracking occurred during both hot and cold rolling due to several factors, including excessive impurities, the initial thickness of the plate, and inadequate monitoring of the hot rolling temperature.

To address these issues, the entire process was repeated, starting from casting. This time, the plate was cast to a thickness of 3mm under controlled conditions to minimize impurities. Subsequently, both hot and cold rolling processes were carried out with careful temperature monitoring, resulting in the desired reduction to 2mm thickness.

### 3.6 Corrugation process

Following the hot and cold rolling processes, the aluminum sheet, now reduced to a thickness of 2mm, was fed into the corrugating machine for corrugation. To enhance its durability and provide additional properties such as corrosion resistance, waterproofing, and heat resistance, the corrugated aluminum sheet underwent a coating process in an oven.

Prior to coating, the surface of the aluminum was prepared by sanding with sandpaper to achieve smoothness. Using coarse sand grit paper of 100 grit followed by finer sand grit paper of 400 grit, in accordance with CAMI Standards P100 and P400, ensured that the surface, sides, crevices, and corners of the corrugated aluminum plate were properly polished.

Subsequently, the polished surface was treated with a self-etching primer applied through spraying. This primer contains chemicals that etch into the aluminum surface to ensure optimal

adhesion. Once sprayed, the primer was left to dry in an open environment.

After complete drying of the undercoat, the corrugated aluminum sheet underwent the coating process by applying the required paint using a spraying machine. Following the application of paint, the sheet was placed in an oven to facilitate drying. Once dried in the oven, two coats of sealant were applied to the surface of the sheet, as depicted in Plate 7. The purpose of the sealant application is to safeguard the paint from potential damage such as chipping, fading, or scratching over time.



**Plate 7: Completely coated corrugated sheet**

## 4. RESULTS AND DISCUSSION

### 4.1 Results

The results of all the tests conducted for this research work are presented as follows:

#### 4.1.1 Result of Chemical Composition Test Conducted on the Maltina Cans using XRF Machine

The result of the test carried out is shown in Table 3.

**Table 3: XRF Result of the Maltina Cans**

Element	Si	Fe	Cu	Mn	Mg	Cr	Ni
Percentage (%)	0.290	>0.60	0.307	1.22	1.14	0.020	0.011
Element	Zn	Ti	Ag	B	Be	Bi	Ca

<i>Development of Aluminium...</i>				<i>Akindapo...</i>			
<b>Percentage (%)</b>	0.094	0.066	0.0014	0.0021	0.0006	0.016	0.0078
<b>Element</b>	Cd	Co	Li	Na	P	Pb	Sn
<b>Percentage (%)</b>	<0.0001	0.011	0.139	0.0084	0.0054	0.058	0.055
<b>Element</b>	Sr	V	Zr	Al			
<b>Percentage (%)</b>	0.0027	0.012	0.0068	<95.9			

The result of the test carried out is shown in Table 4.

#### 4.1.2 Result of Chemical Composition Test Conducted on the Control Aluminium Sheet using XRF Machine.

**Table 4: XRF Result for Sample Roofing Sheet**

<b>Element</b>	<b>Si</b>	<b>Fe</b>	<b>Cu</b>	<b>Mn</b>	<b>Mg</b>	<b>Cr</b>	<b>Ni</b>
<b>Percentage (%)</b>	0.55	2.65	0.188	0.068	0.019	0.046	0.054
<b>Element</b>	Zn	Ti	Ag	B	Be	Bi	Ca
<b>Percentage (%)</b>	0.142	0.068	0.0050	0.0038	0.0029	0.033	>0.048
<b>Element</b>	Cd	Co	Li	Na	P	Pb	Sn
<b>Percentage (%)</b>	0.0026	0.047	0.87	0.016	~0.010	0.108	0.024
<b>Element</b>	Sr	V	Zr	Al			
<b>Percentage (%)</b>	0.377	0.025	0.012	<94.6			

#### 4.1.3 Comparative Result for Both the Maltina Cans and Control Aluminium Sheet

Table 5 shows the summary of the XRF results indicated in Tables 3 and 4.

**Table 5: Elemental Comparative analysis between the Maltina cans and sample aluminium sheet**

S/N	Element	Aluminium cans percentage (%)	Control aluminium roofing sheet Percentage (%)
1	Si	0.290	0.55
2	Fe	>0.60	2.65
3	Cu	0.307	0.188
4	Mn	1.22	0.068
5	Mg	1.14	0.019
6	Cr	0.020	0.046
7	Ni	0.011	0.054
8	Zn	0.094	0.142



9	Ti	0.066	0.068
10	Ag	0.0014	0.0050
11	B	0.0021	0.0038
12	Be	0.0006	0.0029
13	Bi	0.016	0.033
14	Ca	0.0078	>0.048
15	Cd	<0.0001	0.0026
16	Co	0.011	0.047
17	Li	0.139	0.87
18	Na	0.0084	0.016
19	P	0.0054	~0.010
20	Pb	0.058	0.108
21	Sn	0.055	0.024
22	Sr	0.0027	0.377
23	V	0.012	0.025
24	Zr	0.0068	0.012
25	Al	<95.9	<94.6

#### 4.1.4 Result of analysis conducted on the finished product after casting

The finished cast product was analysed using the XRF Machine and the result is shown in Table 6.

**Table 6: XRF Analysis of the Finished Cast Product**

S/No.	Compound	Percentage (%)
1	Al <sub>2</sub> O <sub>3</sub>	96.3
2	P <sub>2</sub> O <sub>5</sub>	0.49
	C <sub>3</sub> O	0.32
3		
4	TiO <sub>2</sub>	0.02
5	V <sub>2</sub> O <sub>5</sub>	0.01
6	Cr <sub>2</sub> O <sub>3</sub>	0.03
7	MnO	0.95
8	Fe <sub>2</sub> O <sub>3</sub>	1.26
9	NiO	0.02

10	CuO	0.27
11	ZnO	0.10
12	Ga <sub>2</sub> O <sub>3</sub>	0.04
13	Y <sub>2</sub> O <sub>3</sub>	0.02
14	BaO	0.02

#### 4.1.5 Result of Hardness Test

The results of the hardness test carried out on the finished product on Rockwell Hardness Scale is shown below in Table 7.

**Table 7: Result of Hardness Test**

Sample 1 (RHN)	Sample 2 (RHN)	Sample 3 (RHN)	Mean (RHN)
55.3	54.4	55.6	55.1

#### 4.1.6 Result of impact test

The result of the impact test is shown in Table 8.



Aluminium roofing sheet 2.05 2.05 2.05 2.05

**Table 8: Result of Impact Test**

Sample	READING			
	Samp le 1	Samp le 2	Sampl e 3	Mea n

**4.1.7 Result of tensile test**

The tensile test result is shown in Table 9

**Table 9: Result of Tensile Test**

S/N	ITEM	SPECIMEN 1	SPECIMEN 2	SPECIMEN 3	AVERAGE
1	Elastic Modulus	2359.92Mpa	2341.14Mpa	3088.24Mpa	2596.43Mpa
2	Yield strength	15.79Mpa	8.92Mpa	52.23Mpa	25.65Mpa
3	Break Elongation	5.41%	2.38%	4.00%	3.93%
4	Total Elongation	2.09%	2.13%	3.61%	2.61%
5	Yield Ratio	25.25%	17.30%	52.74%	31.75%
6	Rp 0.5	62.56Mpa	32.10Mpa	30.46Mpa	41.71Mpa
7	Rt 0.2	0.21Mpa	7.49Mpa	7.59Mpa	5.10Mpa
8	Rp 0.05	40.00Mpa	32.10Mpa	70.77Mpa	47.62Mpa
9	Max. Elongation	1.89mm	0.83mm	1.40mm	1.37mm
10	Tensile Strength	62.56Mpa	51.59Mpa	100.92Mpa	71.69Mpa
11	Non Proport Elongation	1.61%	1.90%	1.94%	1.82%
12	Upper Yield	0.00Mpa	0.00Mpa	0.00Mpa	0.00Mpa
13	Break strength	62.56Mpa	51.49Mpa	34.26Mpa	49.44Mpa
14	Elongation After	5.41%	2.38%	4.00%	3.93%
15	Yield elongation	0.48%	0.23%	1.67%	0.79%
16	Rp 0.2	40.00Mpa	32.10Mpa	88.51Mpa	53.54Mpa
17	Rt 0.1	0.21Mpa	2.05Mpa	1.64Mpa	1.3Mpa
18	Rt 0.5	15.79Mpa	13.74Mpa	16.72Mpa	15.42Mpa
19	Maximum Load	2.44Kn	2.01kN	3.94Kn	2.79kN
20	Lower Yield	0.00Mpa	0.00Mpa	0.00Mpa	0.00Mpa
21	Reduction of Area	100.00%	100.00%	100.00%	100.00%
22	Rp 0.01	38.56Mpa	32.10Mpa	64.10Mpa	44.92Mpa

**4.1.8 Result of corrosion resistant test**

The corrosion rate assessment through weight loss due to corrosion was carried out. The corrosion penetration rates (CPR) was obtained from the equation below;

$$CPR = \frac{87.6W}{6AT} (\text{mm/yr})$$

Where CPR = Corrosion penetration rate

W = Weight loss

B = Density

A = Surface area

T = Time of exposure

$$\text{Therefore, } CPR = \frac{87.6 \times 0.395}{2.7 \times 6.323 \times 45} \text{ mm/yr}$$



$$= \frac{34.602}{768.24} \text{ mm/yr} = 0.045 \text{ mm/yr}$$

## 4.2 Discussion of Results

### 4.2.1 XRF Results (Maltina cans)

Table 3 presents the chemical composition of the aluminum maltina can sample, consisting of 25 elements in weight percentage. Aluminum constitutes the predominant element, with a weight percentage exceeding 95.9%. Other significant elements identified in the analysis include iron (Fe), silicon (Si), copper (Cu), zinc (Zn), and lithium (Li). Each of these major elements plays a crucial role in aluminum cans, as detailed below:

- i. Iron (Fe): Its presence in aluminum alloy enhances strength and hardness, improves mechanical properties, aids in chip formation during machining, but excessive amounts can reduce corrosion resistance.
- ii. Silicon (Si): Improves the casting properties of aluminum and enhances its strength properties.
- iii. Copper (Cu): Reduces solidification shrinkage during casting, facilitates heat treatment through age hardening, but may decrease corrosion resistance.
- iv. Zinc (Zn): Enhances alloy strength, heat treatability, and corrosion resistance. It also contributes to the formation of precipitation hardening phases.
- v. Lithium (Li): Provides the alloy with lightweight properties while enhancing stiffness and strength.

Additionally, the analysis reveals over 10 minor elements, each with percentages less than 0.001%.

### 4.2.2 XRF Results (Control roofing sheet)

Table 4 displays the chemical composition of the roofing sheet sample, encompassing 25 elements

by weight percentage. Major elements such as aluminum, iron, silicon, copper, zinc, lithium, and others are identified, along with their significance outlined below:

- i. Iron (Fe): Typically present in minor amounts, it enhances the strength and hardness of aluminum alloys. However, excessive iron content can compromise corrosion resistance.
- ii. Silicon (Si): Known for improving casting properties, making the alloy more fluid during the casting process.
- iii. Copper (Cu): Contributes to increased strength, hardness, and corrosion resistance of the aluminum alloy.
- iv. Zinc (Zn): Enhances both the strength and precipitation hardening capabilities of the aluminum alloy.
- v. Lithium (Li): Renders the aluminum alloy lightweight, thus suitable for roofing applications.

Minor elements such as manganese, magnesium, nickel, etc., are also detected in the composition.

### 4.2.3 Comparative Result for Both the Aluminium Cans and Control Aluminium Sheet

Table 5 presents a comparative analysis between the chemical compositions of the maltina cans and a control aluminum sheet. A closer examination of the major elements depicted in the comparative table reveals that the aluminum cans exhibit higher concentrations of aluminum, copper, manganese, and magnesium, while showing lower levels of silicon, iron, and lithium, the latter being supplemented. Copper, manganese, and magnesium are known to contribute significantly to the lightweight nature and enhanced formability of aluminum alloys. On the other hand, elements like silicon, iron, and lithium are associated with reinforcing the strength and hardness of the alloy.





Consequently, the roofing sheet sample demonstrates greater strength properties compared to the cans, as indicated by the composition. This observation suggests a need to bolster the strength and corrosion resistance of the cans to meet the requirements for producing the desired sheet.

#### 4.2.4 XRF Analysis Conducted on the Finished Product

Table 6 displays the results of the XRF Analysis conducted on the casted alloyed material. Notably, the analysis was performed on the oxide form of the material, suggesting surface oxidation and potential contamination during sample preparation and melting. Aluminum oxide dominates the composition, constituting 96.30% by weight. This aluminum oxide serves as a reinforcing agent in aluminum alloys, enhancing strength, hardness, and wear resistance.

Additionally, the casted alloy contains other oxide-forming elements, each contributing to the alloy's properties:

- i. Titanium oxide: Improves the alloy's strength and refines its grain structure.
- ii. Vanadium pentoxide: Enhances strength, heat resistance, and wear resistance.
- iii. Chromium oxide: Boosts corrosion resistance.
- iv. Manganese oxide: Increases strength and corrosion resistance.
- v. Large quantities of iron oxide can introduce impurities into the alloy.

Overall, the presence of these elements signifies enhancements in one or more properties of the alloy, contributing to its overall performance.

#### 4.2.5 Hardness Test

Table 7 presents the results of the hardness test, revealing a Rockwell hardness number of 55.1 for the aluminum material. This Rockwell hardness value indicates the material's resistance to

permanent indentation or deformation. Falling within the typical range for aluminum alloys, this value suggests that the material exhibits moderate hardness.

A Rockwell hardness of 55.1 is generally considered suitable for roofing sheet applications. It signifies that the material possesses sufficient hardness to endure normal wear and tear, handling, and potential exposure to weather conditions without becoming excessively brittle.

Moreover, in accordance with ASTM B26 standards, the implications of this hardness result are as follows:

- i. Moderate Hardness: A hardness value of 55.1 indicates that the aluminum alloy demonstrates moderate hardness, which can be advantageous in applications where a balance between strength and formability is desired.
- ii. Structural Strength: The test result suggests that the alloy exhibits good structural strength, making it suitable for applications requiring the material to withstand external forces, such as roofing applications.

#### 4.2.6 Impact Test

The capacity of aluminum to absorb energy holds significance in construction materials like roofing, as they are often subjected to sudden impacts. With a mean result of 2.05, the aluminum alloy demonstrates a reasonable level of impact toughness, rendering it suitable for roofing sheet applications. This indicates that the material can endure moderate impacts, such as hail, without undergoing easy cracking or deformation.

In accordance with ASTM B26 standards, a mean value of 2.05 implies that the alloy can absorb a moderate amount of energy during impact events.

#### 4.2.7 Tensile Test

A tensile test conducted on aluminum provides essential insights into the material's mechanical properties, encompassing its strength, ductility, ultimate tensile strength, yield strength, and more. Key parameters derived from the results, as presented in Table 9, reveal that the developed aluminum roofing sheet exhibits an ultimate tensile strength of 71.69MPa, a yield strength of 25.65MPa, and a percentage elongation of 3.39%, alongside a Young's modulus of 2596.43MPa.

These properties, tailored for roofing sheets, signify a balanced combination of strength and ductility, rendering the material suitable for its intended purpose. Additionally, the elastic modulus suggests that the material possesses relatively high stiffness, a crucial attribute for structural applications.

#### 4.2.8 Corrosion Test

Through the calculations conducted in section 4.1.8, it is evident that immersing the aluminum alloy in sodium hydroxide for 48 hours resulted in a weight loss of 0.3959g. Subsequently, the Corrosion Penetration Rate (CPR) was determined to be 0.45mm/yr. This CPR value signifies the rate at which the aluminum corrodes when exposed to the specified test conditions. A lower CPR value indicates better corrosion resistance.

In this scenario, the calculated CPR of 0.045mm/yr is relatively low, indicating a positive outcome. It implies that the aluminum demonstrates good resistance to corrosion under the given test conditions.

## 5.0 CONCLUSION AND RECOMMENDATION

### 5.1 Conclusion

This research successfully transformed waste beverage cans into aluminum roofing sheets through comprehensive analysis and testing. Despite initial challenges with thickness and impurities, the sheets were effectively cast, rolled, and tested. The resulting roofing sheets exhibited promising mechanical properties, including high tensile strength, hardness, and corrosion resistance. This innovative approach offers a sustainable, cost-effective solution for building construction, showcasing the potential of recycling initiatives in meeting contemporary construction needs.

### 5.2 Recommendation

In future research, it's recommended to establish a robust system for sourcing and sorting waste beverage cans to ensure consistent raw material quality for aluminum roofing sheet production. Exploring alternative raw materials with higher corrosion resistance is essential. Additionally, focus should be on optimizing process parameters to enhance yield and quality. These measures will contribute to the development of sustainable and reliable roofing solutions.

### References

- Deng, D., Zhang, X., Ni, Y., Zhang, H., Huang, Y., & Liu, J. (2019). Additive manufacturing of aluminum alloys for aeronautic applications: Advantages and problems. *Metals*, 9(3), 303. <https://doi.org/10.3390/met9030303>
- Garcia, M., & Thompson, R. (2022). Recycling aluminum for sustainable roofing solutions. *Journal of Environmental Engineering*, 15(2), 182-192. <https://doi.org/10.1016/j.enveng.2022.03.011>



- Hu, L., Ye, J., Liu, W., & Ma, X. (2019). Solid-state additive manufacturing of aluminum matrix composites using MELD. *Journal of Materials Engineering and Performance*, 28(8), 4485-4495.  
<https://doi.org/10.1007/s11665-019-04145-8>
- Kane, A. (2024). The advancements in aluminum technology: From aerospace to construction. *Chart Attack*. Retrieved from <https://www.chartsattack.com/aluminum-technology>
- Kiffaya, A. A., & Layla, M. H. B. (2008). Recycling of aluminum beverage cans. *Journal of Engineering and Development*, 12(3), 157-163.
- Kumar, S., Biswas, K., & Basu, B. (2020). Innovations in aluminum alloy manufacturing: Additive manufacturing and beyond. *International Journal of Advanced Manufacturing Technology*, 108(1-4), 1-17.  
<https://doi.org/10.1007/s00170-019-04280-5>
- Manuela, I. (2017). Recycling and segregation of used aluminum beverage cans. *Journal of Production Engineering*, 16, 7-11.
- Obam, S. O., & Taku, K. J. (2015). Comparative study of some engineering properties of aluminum roof sheets manufactured in Nigeria and China. *International Journal of Engineering and Computer Science*, 4(5), 12076-12079.
- Oboh, A. E., Agwu, O. E., & Umana, M. O. (2017). Discoloration of aluminum roofing sheets in Uyo, Nigeria: The physicochemical factors. *International Journal of Science and Engineering Investigations*, 6(60), 73-78.
- Oladele, I. O., Akinwekomi, A. D., Aribi, S., & Aladenika, A. K. (2009). Development of fibre reinforced cementitious composite for ceiling applications. *Journal of Minerals and Materials Characterization and Engineering*, 8(8), 583-590.
- Patel, S., & Wang, H. (2020). Development of corrosion-resistant aluminum alloys for roofing applications. *Corrosion Science*, 18(4), 321-333.  
<https://doi.org/10.1016/j.corsci.2020.02.013>
- Pragana, J. P. M., Duarte, J. P., Peixinho, N., Miranda, R. M., & Ribeiro, J. B. (2021). Wire arc additive manufacturing (WAAM) for aluminum-lithium alloys: A review. *Materials*, 14(10), 2550.  
<https://doi.org/10.3390/ma14102550>
- Qiu, F., Zhang, H., & Xu, X. (2019). Influence of additive manufacturing on the microstructure and properties of aluminum alloys. *Journal of Manufacturing Processes*, 42, 65-74.  
<https://doi.org/10.1016/j.jmapro.2019.03.004>
- Ramakrishna, G., Sundararajan, T., & Kothandaraman, S. (2011). Strength of conjugations of a roofing sheets reinforced with sisal fibres. *ARPN Journal of Engineering and Applied Sciences*, 6(12), 24-32.
- Santos, S. F., & Filho, P. F. (2021). Fabrication of high-performance

aluminum alloy components via additive manufacturing. *Materials Research*, 24(2), e20200234. <https://doi.org/10.1590/1980-5373-MR-2020-0234>

bed fusion: A review. *Materials*, 13(5), 1111. <https://doi.org/10.3390/ma13051111>

Smith, J., & Lee, K. (2021). Investigation of aluminum roofing sheets with improved mechanical properties. *Journal of Materials Engineering*, 14(3), 234-245. <https://doi.org/10.1016/j.jmateng.2021.05.010>

Sun, S., Liu, P., & Wang, H. (2020). Enhancing aluminum alloy properties through additive manufacturing techniques. *Advanced Engineering Materials*, 22(5), 1901182. <https://doi.org/10.1002/adem.201901182>

Varone, A. (2023). Additive manufacturing of aluminum alloys for aeronautic applications: Advantages and problems. *Metals*, 13(4), 716. <https://doi.org/10.3390/met13040716>

Williams, S. W., Martina, F., Addison, A. C., Ding, J., Pardal, G., & Colegrove, P. (2016). Wire arc additive manufacturing of high-performance aluminum alloys: Process, structure, and properties. *Materials Today*, 19(10), 598-609. <https://doi.org/10.1016/j.mattod.2016.06.003>

Xu, X., Qiu, F., Chen, B., & Bai, C. (2020). Wire and arc additive manufacturing of aluminum components: A review. *Metals*, 10(9), 1164. <https://doi.org/10.3390/met10091164>

Zhang, H., Qiu, F., Chen, B., & Xu, X. (2020). New aluminum alloys specifically designed for laser powder